

行政院國家科學委員會專題研究計畫 期中進度報告

Donor/Acceptor 共軛高分子系統：理論分析、合成、及元件應用(2/3)

期中進度報告(精簡版)

計畫類別：個別型

計畫編號：NSC 95-2221-E-002-154-

執行期間：95年08月01日至96年07月31日

執行單位：國立臺灣大學高分子科學與工程學研究所

計畫主持人：陳文章

報告附件：出席國際會議研究心得報告及發表論文

處理方式：期中報告不提供公開查詢

中華民國 96 年 05 月 24 日

行政院國家科學委員會補助專題研究計畫 成果報告
 期中進度報告

Donor/Acceptor 共軛高分子系統: 理論分析、合成、及元件應用(2/3)

計畫類別： 個別型計畫 整合型計畫

計畫編號：NSC-95-2221-E-002-154

執行期間：95 年 8 月 1 日至 96 年 7 月 31 日

計畫主持人：陳文章

計畫參與人員：李文亞、吳文中、劉振良、鄭凱方、童宜峙、闕居振

成果報告類型(依經費核定清單規定繳交)： 精簡報告 完整報告

本成果報告包括以下應繳交之附件：

赴國外出差或研習心得報告一份

赴大陸地區出差或研習心得報告一份

出席國際學術會議心得報告及發表之論文各一份

國際合作研究計畫國外研究報告書一份

處理方式：除產學合作研究計畫、提升產業技術及人才培育研究計畫、
列管計畫及下列情形者外，得立即公開查詢

涉及專利或其他智慧財產權， 一年 二年後可公開查詢

執行單位：國立台灣大學高分子所

中 華 民 國 96 年 5 月 24 日

中文摘要

本研究將討論 fluorene-based、fluorene-based donor-acceptor-donor、與 thiophene-based donor-acceptor 交替式共軛高分子之光電特性與元件應用。本研究成功地釐清電子受體結構對於 fluorene-based donor-acceptor-donor 共軛高分子電子光電特性的影響。研究成果發現隨著電子受體強度不同，能隙會有著 $\text{PFDTTP} < \text{PFDTBT} < \text{PFDDTQ} < \text{PFTT}$ ，此順序與螢光光譜波峰和場效應電晶體電洞遷移率的趨勢相反。而在 thiophene-based donor-acceptor 交替式共軛高分子之研究方面，利用 Still-coupling 反應成功地合成出低能隙 thiophene(TH)- thienopyrazine(TP)共軛高分子。隨著 thiophene 與 TP 比例改變，我們建立出其高分子光電特性與結構之間的關連性，並發現能隙會隨著 thiophene 比例增加而降低，此結果也與理論計算分析相同。其中由於 PTHTP-12C 擁有最強的分子內電荷轉移而得到最低的能隙 0.97 eV。在理論計算中，P (TH-alt-TP) 的有效載子質量非常小，因此可預見 thiophene(TH)- thienopyrazine(TP)共軛高分子將可以成為極具潛力的場效應電晶體材料。在分子發光二極體方面，利用 fluorene-based 共軛高分子摻混的方式來研討電子受體結構與對於高分子特性的影響，並且來製備成白光發光二極體。發現 **FQTP1** (PF:PFQ:PFTP = 98.50:1.00:0.50, weight ratio)與 **FBTTP1** (PF:PFBT:PFTP = 99.65:0.05:0.30, weight ratio)皆可達到白光，且 **FBTTP1** 發光效率可達到 1.89 cd/A。本年度執行本計畫共發表 9 篇 SCI 期刊論文(*Langmuir* (1), *Adv. Funct. Mater.* (1), *Macromolecules* (1), *Macromol. Rapid Commun.* (2), *J. Polym. Sci. Polym. Chem.*(3), *J. Polym. Sci. Polym. Phys.*(1))。

關鍵詞：donor-acceptor 共軛高分子、發光二極體、薄膜電晶體。

Abstract

The optoelectronic and device characteristics of fluorene-based, fluorene-based donor-acceptor-donor and thiophene-based donor-acceptor copolymers were investigated. The experimental results suggested that the acceptor structures of fluorene based donor-acceptor-donor conjugated copolymers significantly affected on their electronic, optoelectronic, and FET characteristics. The order of the band gap is $\text{PFDTTP} < \text{PFDTBT} < \text{PFDDTQ} < \text{PFTT}$, which is on the reverse trend of luminescence and FET mobility. Five small band gap thiophene(TH)-thienopyrazine(TP) conjugated copolymers were successfully synthesized by Stille-coupling reaction. The polymer structures consisted of one to four thiophene rings with TP of different side group provide systematical investigation on the structure-electronic property relationship. Both experimental and theoretical results suggest that the band gaps reduce as the thiophene moiety increased. The relatively small optical (0.97 eV) and electrochemical (0.78 eV) band gaps of poly PTHTP-C12 suggest the importance of intramolecular charge transfer. The theoretical results also suggest that the poly(TH-alt-TP) could have a relatively small effective mass for field transistor applications. The relatively small

theoretical effective mass of poly(TH-alt-TP) also suggests its potential applications for field transistor applications. Our study demonstrates the tuning of the electronic properties of small band gap copolymers by the thiophene content and the resulted geometry variation. Such Polymers could be potentially used for near-infrared electronic and optoelectronic devices. For the light-emitting diodes, the effects of acceptor structures on the electronic and optoelectronic properties of conjugated polymer blend were studied. The white-emitting electroluminescence was achieved with by PF blending a relatively small amount of acceptors, such as FQTP1 (PF:PFQ:PFTP = 98.50:1.00:0.50, weight ratio) and FBTTP1 (PF:PFBT:PFTP = 99.65:0.05:0.30, weight ratio). The luminance yield and maximum external quantum efficiency of the white-light emitting diode based on the ternary blend FBTTP1 as emissive layer were 1.89 cd/A and 0.47%, respectively. 12 SCI Journal papers based on this projected have either been published or in press: (*Langmuir* (1), *Adv. Funct. Mater.* (1), *Macromolecules* (1), *Macromol. Rapid Commun.* (2), *J. Polym. Sci. Polym. Chem.*(3), *Macromol. Chem. Phys.* (2), *J. Polym. Sci. Polym. Phys.*(1), *J. Polym. Res.* (1)) °

Keywords: donor-acceptor conjugated polymers, light-emitting diodes, thin-film transistors.

Contents

| | |
|---|----|
| 中文摘要..... | 2 |
| Abstract..... | 2 |
| 1. Introduction..... | 5 |
| 2. Objective..... | 5 |
| 3. Experimental..... | 5 |
| 4. Results and discussions..... | 7 |
| 4.1. Photophysical and electroluminescent properties of ternary fluorene-acceptor polymer blends..... | 7 |
| 4.2. Effects of Acceptors on the Electronic and Optoelectronic Properties of Fluorene Based Donor-Acceptor-Donor Copolymers..... | 9 |
| 4.3. Small Band Gap Conjugated Polymers Based on Thiophene-Thienopyrazine Copolymers..... | 12 |
| 5. Conclusions..... | 15 |
| 6. Reference..... | 16 |
| 7、計畫結果自評..... | 27 |
| 8、本年度經由本計畫經費支持所發表期刊論文目錄..... | 27 |

1. Introduction

Donor-acceptor conjugated polymer systems have emerged as promising candidates for flexible organic electronic devices since their electronic and optoelectronic properties of donor-acceptor copolymers could be efficiently manipulated by controlling intramolecular charge transfer (ICT). The studied polymer systems included alternating or random copolymers, polymer blends, and multilayer in the application areas of polymer light-emitting diodes,^[1-7] Field effect transistors (FET)^[8-10], and photovoltaic device.^[11]

Several different donor-acceptor conjugated polymers have been reported in the literature. We are particularly interested in the thiophene-acceptor, fluorene-acceptor and fluorene-donor-acceptor-donor conjugated polymers due to the judicious structural modification and flexibility on tuning the electronic and optoelectronic properties for device applications.

2. Objective

Donor-acceptor conjugated polymer can effectively increase the efficiency of device, such as polymer light-emitting diodes, field-effect transistors, and photovoltaic devices. However, there are some following problems: (1) the absence of analysis of theoretic geometries and electronic structures of copolymers; (2) the absence of studies of various donor-acceptor structures; (3) the lack of knowledge of interface of polymer blends for optoelectronic properties; (4) the lack of applications of field-effect transistor. Therefore, the aim of this project is to investigate EDOT, thiophene, fluorene-based donor-acceptor conjugated copolymers further. The goals of the second-year project are the following two parts: (1) the first part is to synthesize various donor-acceptor conjugated copolymers, and characterize their optoelectronic properties, and build the relationship between chemical structures and optoelectronic properties; (2) PLEDs and field-effect transistors are fabricated with our studied donor-acceptor copolymers.

3. Experimental

3.1. Computational Method

The ground-state geometries and electronic structures of the studied donor-acceptor conjugated polymers were optimized by means of the hybrid density functional theory (DFT) method treated in periodic boundary conditions (PBC) at the B3LYP level of theory (Becke-style three-Parameter Density Functional Theory using the Lee-Yang-Parr correlation functional) with the 6-31G(d) basis set performed on Gaussian03 program package. It was shown that the calculations for conjugated polymers using the hybrid B3LYP functional coupled with PBC were in excellent agreement with the experimental values.

3.2. Materials

All reagents were purchased from Aldrich (Missouri, USA) or Acros (Geel, Belgium) and used

without further purification. Ultra-anhydrous solvents used in the reactions were purchased from Tedia (Ohio, USA), Echo, and Merck without further purification unless noted.

3.3. General procedure of Polymerization

Scheme 1 is the synthesis process of thiophene, thienopyrazine, and donor-acceptor-acceptor monomers. Our studied copolymers were synthesized via a Suzuki coupling reaction or Stille coupling reaction, as shown in scheme 2.

3.4. Characterization

UV-Visible absorption and photoluminescence (PL) spectra were recorded on a Jasco model UV/VIS/NIR V-570 spectrometer and Fluorolog-3 spectrofluorometer (Jobin Yvon), respectively. Films used for the PL efficiency measurement were drop-coated from THF solution onto quartz substrates (*ca.* 1 wt %). PL efficiencies of polymer films on quartz substrates were measured using fluorolog 3 in combination with integrating sphere with 380 nm excitation. The refractive index and thickness of the studied polymer film were measured by the F20 Thin Film Measurement system (Filmetrics, Inc., CA, USA). The electrochemical properties of the polymer films were investigated on a Princeton Applied Research Model 273A Potentiostat/Galvanostat with a 0.1 M acetonitrile (99.5+%, Tedia) solution containing tetrabutylammonium tetrafluoroborate (TBABF₄) (Fluka, >99.9%) as the electrolyte.

3.5. Device Fabrication and Testing

Polymer Light-Emitting diodes. The electroluminescent (EL) devices were fabricated on indium-tin oxide (ITO) coated glass substrate. Onto the ITO glass a layer of poly(ethylene dioxythiophene):poly(styrene sulfonate) (PEDOT:PSS), which was formed by spin-coated from its aqueous solution (Baytron P 8000, Bayer). The emissive layer was spin-coated at 1500 rpm from the corresponding p-xylene solution (1.5 wt%). Under high vacuum, a layer of Ca (10 nm) was vacuum deposited as cathode and a thick layer of Ag (100 nm) was deposited subsequently as the protecting layer. Current-Voltage characteristics were measured with a computerized Keithley 2400 source measure unit. The luminance and CIE coordinate of device were measured with Konica-Minolta Chroma Meter CS-100A. The EL spectrum of device was recorded on Fluorolog-3 spectrofluorometer (Jobin Yvon).

Thin Film Transistors. The thin film transistors were fabricated from the four fluorene alternating copolymer with a bottom-contact configuration on the p-doped silicon wafers. A thermally grown 200 nm SiO₂ used as the gate dielectric with a capacitance of 17 nF/cm². Aluminum was used to create a common bottom-gate electrode. The source/drain regions were defined by a 10 nm thick chromium adhesion layer and a 100 nm thick gold contact electrode through a regular shadow mask, and the channel length (L) and width (W) were 25 and 1500 μm, respectively. Afterward, the substrate was modified with hexamethyldisilazne (HMDS, Fluka, 98%) as silane coupling agents. Output and transfer characteristics of the OTFT devices were

measured using Keithley 4200 semiconductor parametric analyzer. All the prepared procedures and electronic measurements were performed in ambient atmosphere.

4. Results and discussions

4.1. Photophysical and electroluminescent properties of ternary fluorene-acceptor polymer blends.

Polymer based white-light-emitting-devices (WLEDs) have been extensively studied recently due to their potential applications in low-cost lighting. Here, we investigated the potential of using the polyfluorene ternary blends to obtain the white emission. In order to obtain white emission, the emission from all of the three components is required and thus compositions of PFQ (or PFBT) and PFTP were controlled to ensure incomplete energy transfer.

The photophysical properties and electroluminescence characteristics of PF-based polymer blends with the components were investigated in this study. The chemical structures and synthesis of the studied poly(fluorene-acceptor) are shown in Scheme 2, including blue-emitting poly[2,7-(9,9'-dihexylfluorene)] (PF), green-emitting poly[2,7-(9,9'-dihexylfluorene)-alt-5,8-quinoxaline] (PFQ), yellow-emitting poly[2,7-(9,9'-dihexylfluorene)-alt-4,7-(2,1,3-benzothiadiazole)] (PFBT), and red-emitting poly[2,7-(9,9'-dihexylfluorene)-alt-5,7-(thieno[3,4-b]pyrazine)] (PFTP). Two kinds of ternary blends, PF/PFQ/PFTP (named as **FQTP**), and PF/PFBT/PFTP (named as **FBTTP**) were investigated to realize white-light emission by tuning the compositions of polyfluorene copolymers with blue, green (yellow), and red emission. Both the photoluminescence (PL) and electroluminescence (EL) of these PF-based polymer blends with different compositions were characterized to realize the effects of component and composition of polymer blends on the energy-transfer processes.

Figure 1 shows the PL spectra of ternary blends (a) **FQTP1~6** and (b) **FBTTP1~6** in solid-state films excited at the wavelength of 380 nm, of which the corresponding emission maxima ($\lambda_{\max}^{\text{PL}}$) are summarized in Table 1. With the addition of PFQ (or PFBT) and PFTP into PF, energy transfers from PF to PFQ (or PFBT) and then from PFQ (or PFBT) to PFTP are observed. The extent of energy transfer is in proportional to the composition of PFQ (or PFBT) and PFTP. Therefore, tuning of PL spectra could be realized by controlling the composition of these polymer blends. In particular, simultaneous emission from all of the three components is required to obtain white emission. Through precise control of the composition of these polymer blends, incomplete energy transfer between these PF-based polymers ensures simultaneous emission from these polymers. For example, the PL spectra of **FQTP6** and **FBTTP6** show simultaneous emission from their components with similar intensity.

The content of PFQ (1-5 wt%) in the ternary blend of **FQTP** required to transfer energy to

PFTP is higher than that of PFBT(0.05-0.5 wt%) in **FBTTP**. This indicates that the energy transfer from PFBT to PFTP is more efficient than that from PFQ to PFTP. By taking **FQTP3** and **FBTTP6** as an example, the PL spectra of these two ternary blends show the PFTP emission with similar intensity. However, the contents of PFBT and PFTP in **FBTTP6** are much lower than those of PFQ and PFTP in **FQTP3**, indicating more efficient energy transfer from PFBT to PFTP. The Förster radii for the energy transfer from PFQ to PFTP and from PFBT to PFTP are 6.5 and 7.3 nm, respectively. The larger Förster radius for the energy transfer from PFBT to PFTP indicates more efficient energy transfer. This could be attributed to the better overlap between the emission of PFBT and the absorption of PFTP than that between the emission of PFQ and the absorption of PFTP, as shown in Figure 1(c). In addition, the overlap integrals for the energy transfer from PFQ to PFTP and from PFBT to PFTP are 3.7×10^{-12} and $7.3 \times 10^{-12} \text{ M}^{-1} \text{ cm}^3$, respectively, which also suggests more efficient energy transfer from PFBT to PFTP.

Electroluminescence of PF-based ternary blends

EL devices with the ternary blends of **FQTP** and **FBTTP** as emissive layers were fabricated with structure of ITO/PEDOT:PSS/emissive layer/Ca:Ag. Figure 2 shows the EL spectra of the devices with the ternary blends of (a) **FQTP** and (b) **FBTTP** as emissive layers, of which the emissive maxima ($\lambda_{\text{max}}^{\text{EL}}$) are listed in Table 2. Although the extent of energy transfer from PF to acceptor is in proportional to the compositions of PFQ (or PFBT) and PFTP, respectively, the EL spectra of these ternary blends are quite different from their corresponding PL spectra. It could be attributed to the differences in the recombination zone for photo- and electric excitation in EL, as described previously. The (HOMO, LUMO) levels of PF and PFTP are (-5.39, -2.44) and (-5.13, -3.33) eV, respectively. The higher HOMO level and lower LUMO level of PFTP than those of PF suggest that PFTP serves as both efficient hole and electron traps in these ternary blends. The more intense green emission from PFQ (or yellow emission from PFBT) and red emission from PFTP in EL were observed as compared to their corresponding PL spectra due to the charge trapping mechanism. Thus, the compositions of PFQ (or PFBT) and PFTP required to ensure incomplete energy transfer and simultaneous emission from all of the three components are much smaller in EL than those in PL. As a result, simultaneous emission from all the three components in EL was realized either with **FQTP1** or **FBTTP1**. The higher composition of PFQ (or PFBT) and PFTP in the ternary blend would result in more complete energy transfer and thus emission from only PFQ (or PFBT) and/or PFTP, such as **FQTP6** and **FBTTP6**. The CIE 1931 coordinates of these devices were measured with Konica-Minolta Chroma Meter CS-100A under the condition of maximum luminance, of which the corresponding data are summarized in Table 2. The CIE 1931 coordinates of ternary blends **FQTP1** and **FBTTP1** are (0.328, 0.310) and (0.320, 0.327), respectively, which are almost identical to standard white emission at (0.33, 0.33). By comparing the two white-light-emitting diodes (WLEDs) based on the ternary blends of **FQTP1** and **FBTTP1**, the compositions of acceptors in **FBTTP1** are much lower than those in

FQTP1. This could be attributed to the following three possible mechanisms. First, PFBT is a better electron trap than PFQ due to the lower LUMO level of PFBT than that of PFQ. Second, the Förster energy transfer from PFBT to PFTP is more efficient due to the better matching between the emission of PFBT and absorption of PFTP. Finally, the difference in the emissive colors of PFQ and PFBT is also important in designing the WLED.

The EL characteristics of the devices with the ternary blends as emissive layers are summarized in Table 1. The maximum luminance yield and EQE decrease with increasing content of **PFTP** both in the ternary blends of the **FQTP** and **FBTTP**. This is probably attributed to the low PL and EL efficiency of **PFTP** due to intramolecular charge transfer and heavy-atom effect as mentioned in previous section. The brightness of WLEDs based on ternary blends **FQTP1** and **FBTTP1** under the condition of maximum luminance yield are 326 and 1360 cd/m², respectively. The maximum luminance yield (cd/A) and maximum EQE (%) of WLEDs based on **FQTP1** and **FBTTP1** are (0.45, 0.13) and (1.88, 0.47), respectively. In spite of WLEDs based on single PF copolymer or doped with phosphorescent materials,^{16,32} the brightness and efficiency of WLEDs based on **FBTTP1** are comparable or even higher than the WLEDs based on **PF**-based polymer blends reported recently. The performance of WLEDs based on ternary **FQTP1** and **FBTTP1** shows bright and efficient white emission were achieved without dyes or phosphorescent materials involved.

4.2. Effects of Acceptors on the Electronic and Optoelectronic Properties of Fluorene Based Donor-Acceptor-Donor Copolymers

FET based Thiophene- or fluorene-based donor-acceptor conjugated polymers have been explored by several groups and us recently. The studied thiophene-acceptor conjugated polymers either exhibit p-type or ambipolar mobility. The above studies suggested that the molecular weight, morphology, and acceptor strength played important roles in the FET characteristics. High hole or electron mobility was also observed in fluorene-based conjugated polymers. However, the effects of various acceptor structures on the FET mobility of fluorene based donor-acceptor conjugated copolymers have not been fully explored yet.

In this study, four fluorene-based conjugated copolymers were synthesized to explore the effects of acceptor structures on the electronic, optoelectronic, and FET characteristics. The chemical structures and synthesis of the studied polymers are shown in Scheme 3, including poly[2,7-(9,9-dihexylfluorene)-alt-2,2':5,2''-terthiophene] (**PFTT**), poly[2,7-(9,9'-dihexylfluorene)-alt-2,3-dimethyl-5,7-dithien-2-yl-quinoxaline] (**PFDDTQ**), poly[2,7-(9,9'-dihexylfluorene)-alt-4,7-dithien-2-yl- 2,1,3-benzothiadiazole] (**PFDTBT**) and poly[2,7-(9,9'-dihexylfluorene)-alt-2,3-dimethyl-5,7-dithien-2-yl-thieno[3,4-b] pyrazine] (**PFDDTTP**). The studied acceptors included quinoxaline (**Q**), 2,1,3-benzothiadiazole (**BT**) and thieno[3,4-b]pyrazine (**TP**). The LUMO levels of the **Q**, **BT**, and **TP** are -0.90, -1.81, and -1.41

eV, respectively, which indicates the order of the acceptor strength is **BT** > **TP** > **Q**. Besides, the five or six-member ring of acceptor backbone allows us to investigate the effect of planarity on the properties. Therefore, the effects of acceptor strength, backbone planarity and intramolecular charge transfer on the field effect mobility as well as other photophysical properties could be realized through this study.

Electrochemical and Optoelectronic Properties. Figure 3 shows the optical absorption spectra of the studied copolymers in thin films. The absorption maximum (λ_{\max}) of **PFTT**, **PFDDTQ**, **PFDTBT**, and **PFDDTTP** are 514, 502, 618, and 616 nm, respectively, while the absorption edges are 606, 639, 736, and 738 nm. It indicates that the optical properties could be tuned over a broad range with various acceptors. The band gaps estimated from the absorption edges are in the order of **PFTT** (2.05 eV) > **PFDDTQ** (1.94 eV) > **PFDTBT** (1.69 eV) > **PFDDTTP** (1.68 eV). The lower E_g of the three copolymers than that of **PFTT** suggests the significance of the intramolecular charge transfer between the donor and acceptor. However, the slightly smaller E_g of **PFDTBT** than that of **PFDDTTP** is not consistent with the acceptor strength (**BT**>**TP**>**Q**). It is probably because the **BT** moiety with a six-member ring has a larger torsional angle than the **TP** segment with a five-member ring and results in the reduction of the π -conjugation. The above result also suggests that the backbone planarity and the intramolecular charge transfer of the **TP** and thiophene is probably high than that of **BT** and thiophene. A strong acceptor could reduce the LUMO level and enhancement of intramolecular charge transfer of donor-acceptor conjugated copolymers.^[3, 12] since it induces a resonance structure between a donor and a acceptor moiety, just like $D-A \leftrightarrow D^+=A^-$.

Figure 4 shows the photoluminescence spectra of **PFTT**, **PFDDTQ**, **PFDTBT**, and **PFDDTTP** films, with the corresponding emission maxima of 574, 620, 677, and 736 nm, respectively. The variation of emission peaks shows the same trend as that of optical band gaps. The emissive colors of **PFTT**, **PFDDTQ**, **PFDTBT**, and **PFDDTTP** are yellow, purple, orange, and red, respectively. It indicates the color tuning is practicable by intramolecular charge transfer through incorporating the acceptor moiety into the polymer backbone. The results of optical absorption and photoluminescence also suggest that both the acceptor strength and the backbone structure play important roles on the photophysical properties.

The electrochemical characteristics of the studied polymers investigated by cyclic voltammetry are shown in Figure 5 and listed in Table 2. The HOMO and LUMO levels of the **PFTT** are -5.08 and -3.03 eV, respectively. The HOMO levels of **PFDDTQ** and **PFDTBT** are similar to that of **PFTT** except **PFDDTTP** with a small HOMO level of -4.97 eV. However, the LUMO levels of these copolymers are smaller than that of **PFTT**, which are -3.23, -3.29, and -3.76 eV for **PFDDTQ**, **PFDTBT**, and **PFDDTTP**, respectively. It indicates that the incorporation of the acceptor moiety could increase electron affinity of the prepared copolymers as expected. The electrochemical band gap estimated from the difference between HOMO and

LUMO levels is generally similar to that of optical band gap.

Field-effect Transistor Characteristics. All the FETs fabricated from **PFTT**, **PFDDTQ**, **PFDTBT**, and **PFDDTTP** shown in Figure 6 exhibit typical p-channel transfer characteristics (drain current (I_d) versus drain voltage (V_d) at various gate voltage (V_g)). In the saturation region ($V_d > V_g - V_t$), where V_t is the threshold voltage, I_d can be described by Eq.(1):^[8]

$$I_d = \frac{WC_o\mu_h}{2L}(V_g - V_t)^2 \quad (1)$$

Where μ_h is the hole mobility, W is the channel width, L is the channel length, and C_o is the capacitance of the gate insulator per unit area, respectively. The saturation region mobility of the studied polymers was calculated from the transfer characteristics of OTFTs. The hole mobilities of **PFTT**, **PFDDTQ**, **PFDTBT**, and **PFDDTTP** estimated from Figure 6 and eq.(1) are 2.35×10^{-6} , 5.44×10^{-6} , 4.87×10^{-5} and $5.52 \times 10^{-5} \text{ cm}^2 \text{ v}^{-1} \text{ s}^{-1}$, respectively. Furthermore, the on-off ratio of **PFTT**, **PFDDTQ**, **PFDTBT**, and **PFDDTTP** are 1×10^3 , 1×10^3 , 2×10^4 , and 5×10^3 , respectively. As shown in Table 2, the hole mobility increases with the reduction of band gaps and LUMO levels of these polymers. The relatively smaller surface roughness (root mean square roughness (RMS): 0.48~3.35 nm) of the prepared polymer films shown in Table 2 suggest the good quality films for device applications. Hence, the trend on the hole mobility could be mostly due to the different polymer structures. The present result suggests that the mobility could be successfully enhanced by intramolecular charge transfer since it increases the double bond characteristics between a donor and an acceptor and thus leads to a effective π -conjugation length and enhanced charge transport within a single polymer chain.

The importance of polymer morphology on charge transport characteristics of OTFTs have been demonstrated extensively in the literature. The effects of solvent quality on the surface structure and OTFT characteristics were further studied by AFM and FET measurements. The FET mobilities of **PFDDTTP** based devices prepared from the solvents of THF and 1,2-dichlorobenzene are of 8.00×10^{-7} and $5.52 \times 10^{-5} \text{ cm}^2 \text{ V}^{-1} \text{ s}^{-1}$, respectively, with the on-off ratios of **PFDDTTP** of 6 and 5×10^3 . The nearly two orders of magnitudes on the FET mobility of **PFDDTTP** FET from 1,2-dichlorobenzene solution than that from THF solution suggests the importance of solvent quality on the FET characteristic. The root-mean-square (RMS) roughness of **PFDDTTP** film prepared from THF and 1,2-dichlorobenzene solution is about 120.71 and 0.475 nm, respectively, as shown in the AFM images of Figure 7. The solubility of **PFDDTTP** and boiling point of the two solvents probably explain the above results. The aggregates shown in Figure 7(b) might make ionization potentials of polymers decrease and lead to oxygen doping. Furthermore, the low mobility of the **PFDDTTP** film prepared from the THF solution could be also explained by the limited boundary between the aggregates, which would make the low

degree of charge transport and result in low FET mobility. Although the FET mobility obtained in the study is similar or smaller than that of other fluorene -acceptor conjugated copolymers, it demonstrates the importance of acceptor structure and processing solvent on the FET mobility. Further enhancement on the FET mobility could be achieved by device or process optimization.

4.3. Small Band Gap Conjugated Polymers Based on Thiophene-Thienopyrazine Copolymers

We are particularly interested in the thiophene-acceptor conjugated polymers due to the judicious structural modification and flexibility on tuning the electronic and optoelectronic properties for device applications. The donor-acceptor-donor (D-A-D) copolymers of thiophene-thienopyrazine-thiophene (**TH-TP-TH**) were reported to have a band gap in the range of 1.10-1.60 eV, depending on the side chain of the aromatic ring. Such polymers could have high field effect mobilities, green polymeric electrochromic properties, and potential photovoltaic characteristics. However, the electronic properties of thiophene-thienopyrazine (**TH-TP**) donor-acceptor (D-A) alternating copolymer have not been fully explored yet. The **EDOT-TP** alternating copolymers had been prepared by electrochemical polymerization and showed a relatively small band gap (1.3eV). However, the solution-processible **TH-TP** would be required for flexible electronic and optoelectronic devices. Besides, the fundamental understanding on the geometry and electronic structures of the thiophene-thienopyrazine copolymers with different compositions would be important for their device applications.

In this study, a joint of theoretical and experimental studies on the electronic properties of thiophene-thienopyrazine D-A alternating copolymers are reported. Five different thiophene-thienopyrazine copolymers consisted of thiophene, bithiophene, terthiophene, quaterthiophene moiety with thienopyrazine of different side groups were synthesized by the Stille coupling reaction, as shown in schemes 4. The electronic properties of the prepared copolymers were estimated by the optical absorption and cyclic voltammetry. The theoretical geometry and electronic properties were investigated by the density functional theory (DFT) at the B3LYP level and 6-31G(d) basis set. The theoretical geometry and bond length alternation of the copolymers were analyzed and correlated with their chemical structures. The effects of the copolymer composition on the theoretical electronic properties, including the HOMO level, LUMO level, band gap, and effective mass were also investigated.

The optical absorption spectra of the prepared polymers in chloroform solution and solid thin films are shown Figures 8 and 9, respectively. The corresponding optical absorption properties are summarized in Table 3. The absorption maxima (λ_{\max}) of **PTHTP-C7**, **PTHTP-C12**, and **PBTHTP** are observed at 748, 774, and 610 nm, respectively. On the other hand, the λ_{\max} of **PTHTP-C7**, **PTHTP-C12**, **PBTHTP**, **PTTHTP** and **PQTHTP** solid films are shown at 790, 850, 670, 640 and 590 nm, respectively, which have the corresponding optical

band gaps of 1.07, 0.97, 1.38, 1.66 and 1.78 eV. Note that the optical band gap of **PBTHTP** is in agreement with the similar structure prepared by chemical or electrochemical method as report in the literature (1.0 eV-1.3eV). In the case of **PTHTP-C7**, **PTHTP-C12** and **PBTHTP**, the λ_{\max} of the solid films are 42, 76 and 60 nm red-shifted compared to the corresponding solution spectra, which is probably attributed to the π - π stacking of the polymer chains in the former. The significantly higher λ_{\max} of the above copolymers than that of polythiophene indicates the significant intramolecular charge transfer (ICT) between the electron-donating thiophene moiety and the electron-accepting thieno[3,4b]pyrazine moiety. Note that the λ_{\max} of the non-regioregular poly (thiophene) (**PHT**) in chloroform and solid state films are 448 and 490 nm, respectively. The comparison of the optical absorption properties in Table 1 suggests that the λ_{\max} increases as the thiophene moiety increases but that of the optical band gap shows a reverse trend. It indicates that geometry of the studied polymers is probably varied as thiophene content increases. The **PTHTP-C7** or **-C12** has the chemical structure of alternating \cdots D-A-D-A \cdots structure. As the thiophene moiety in the polymer structure increases, it reduces the acceptor content and results in decreasing the intramolecular charge transfer. Consequently, it enhances the bond length alternation and results in increasing optical band gap. The theoretical analysis will discuss such effects in details later.

The optical absorption of the **PTHTP-C7** film exhibits a board band with the λ_{\max} at 1545 nm after doped with iodine vapor, which is significantly higher than that (790 nm) of the pristine **PTHTP-C7**, as shown in the insert figure of Figure 9. The conductivities of the pristine **PTHTP-C7** and that after I_2 doping were $1.23 \times 10^{-7} \text{ S}\cdot\text{cm}^{-1}$ and $1.95 \times 10^{-5} \text{ S}\cdot\text{cm}^{-1}$, respectively. The low conductivity of the doped **PTHTP-C7** could be due to the low molecular weight polymer.

Electrochemical Properties

The oxidation and reduction potentials of these polymers were investigated by cyclic voltammetry. Figure 10 shows the cyclic voltammograms (CV) diagrams of **PTHTP-C7**, **PTHTP-C12**, and **PBTHTP** and the corresponding electrochemical properties are listed in Table 1. All three copolymers exhibit reversible oxidation but not in the case of reduction. The HOMO levels of the three studied polymers determined by CV are in the range of -4.45 ~ -4.7 eV. The LUMO levels of **PTHTP-C7**, **PTHTP-C12**, and **PBTHTP** are -3.25, -3.92, and -3.21, respectively. The electrochemical band gaps estimated from the gap between LUMO and HOMO are in the trends of **PBTHTP** (1.34 eV) > **PTHTP-C7** (1.20 eV) > **PTHTP-C12** (0.78 eV). Although the values of the above electrochemical band gap are not the same as those of optical band gap, the trend on the three polymers is the same. It again demonstrates the significance of thiophene content on the electronic properties.

Theoretical Analysis on Geometry and Electronic Structures of Thiophene-Thienopyrazine

(TH-TP) alternating Polymers

The calculated optimized geometries and electronic properties of the studied donor-acceptor conjugated polymers without alkyl substituents are listed in Table 4. The effects of bond length alternation (BLA, δ), HOMO, LUMO and band gap (E_g) on the polymer structures are discussed below. Hence, the theoretical results on the geometrical and electronic property of **PTHTP** were different from those reported previously by our group. From Table 2, all the donor-acceptor conjugated polymers show near zero dihedral angles which exhibit the fully coplanar structures. X-ray analysis involving the **TP** moiety also show nearly coplanar structures due to the inter-ring S-N or H-N interaction.

Figure 11 (a) and 7(b) show the optimized geometries of the **PTHTP** and **PTTHTP**, respectively. The optimum geometries of the homopolymers, **PTH** and **PTP**, are the aromatic and quinoid structures, respectively. Copolymerization of 1:1 stoichiometry donor and acceptor moiety, **PTHTP**, favors an aromatic structure, as evidenced by the bond length with π -delocalization within each unit. The bonds of C₁-C₂ (1.395Å), C₂-C₃ (1.395Å), C₃-C₄ (1.406Å) and C₄-C₅ (1.406Å) of Figure 7(a) are suggested to be a double bond while those of C₂-C₂ (1.400Å), C₃-C₃ (1.426Å) and C₄-C₄ (1.436Å) are single bonds, resulting in the slightly aromatic-dominant character. The relative carbon bond lengths of **PTTHTP** shown in Figure 11 (b) also exhibit the aromatic geometry as well. The optimized theoretical results suggest that all copolymers with different donor/acceptor fraction (1:1, **PBTHTP**; 2:1, **PBTHTP**; 3:1, **PTTHTP**; 4:1, **PQTHTP**) are preferred to be aromatic structures. **PTHTP** shows the smallest BLA (δ_D , δ_A) and bridge length (L_B) of all four donor-acceptor conjugated polymers due to the more efficient π -delocalization resulted from significant intramolecular charge transfer. The BLA in **PTH**, **PTHTP** and **PTP** are 0.031(δ_D), 0.005 (δ_D), and 0.026 Å (δ_A), respectively. It suggests that the relaxation of bond length mainly occurs in thiophene unit after incorporating the quinoid-like thienopyrazine unit since the large BLA reduction of **PTHTP** in comparison with that of **PTH**. The BLA in the thiophene moieties of **PTHTP**, **PBTHTP**, **PTTHTP**, and **PQTHTP** are 0.005, 0.016, 0.019, and 0.021 Å, respectively. It indicates that the BLA is enlarged with increasing the thiophene moiety and thus results in the aromatic-dominant structure. Furthermore, the bridge length also shows the same results. The order of the L_B between the thiophene and thienopyrazine is **PTP** < **PTHTP** < **PBTHTP** < **PTTHTP** < **PQTHTP** < **PTH**, as shown in Table 4. The enhanced inter-ring bridge length also explains the tendency of toward aromatic-like structures as increasing the thiophene fraction.

Figure 12 (a) and (b) show the calculated one-dimensional band structures along polymer chain of **PTHTP** and **PTTHTP**, respectively. All the band gap values are derived from the direct transition at $k = 0$ with the highest occupied band and lowest unoccupied band. The order of the obtained theoretical E_g (eV) is **PTHTP** (0.90) > **PBTHTP** (1.21) > **PTTHTP** (1.36) > **PQTHTP** (1.45). The above theoretical band gaps are in a good agreement with those from the experimental results discussed in the optical property section. The theoretical band gap of stable

aromatic **PTH** and quinoid **PTP** from DFT//B3LYP/6-31G(d) theory shown in Table 4 is 2.07 and 1.31 eV, respectively, which are very close to the experimental band gap of 2.0 (optical) and 0.95 (electrochemical) eV. The deviation is probably attributed to the interchain interaction in polymer thin film, which is not considered for an isolated single polymer chain in our theoretical calculations. The order of band gap is in the same trend of the BLA and suggests that the BLA contributes significantly to the order of E_g . However, a slightly larger band gap of **PTHTP** and **PQHTP** than **PTP** is mainly due to the large bond length alternation.

The electron effective mass are calculated on the upper valence band or lower conduction band, which is a good parameter for predicting the hole or electron ability. As shown in Table 4, the relatively smaller band gap and effective mass of the **PTHTP** compared to other polymers facilitating the π -electron delocalization make more potential applications for transparent conductor, photovoltaic devices and thin film transistors.

5. Conclusions

The optoelectronic and device characteristics of fluorene-based, fluorene-based donor-acceptor-donor and thiophene-based donor-acceptor copolymers are investigated. The chemical structures and compositions of the acceptor in the polymer blend significantly affect the energy transfer and the resulted luminescence characteristics. The ternary blends composed of PF, PFQ (or PFBT), and PFTP are also explored for the potential white light-emitting diodes(WLED). The luminance yield and maximum external quantum efficiency of the white-light emitting diode with ternary blend **FBTTP1** as emissive layer are 1.89 cd/A and 0.47%, respectively. The present study suggests that the polymer blend approach is a potential approach for enhancing luminescence characteristics or color tuning in LEDs.

In this study, we have also successfully addressed the role of acceptor structures of fluorene based conjugated copolymers on their electronic, optoelectronic, and FET characteristics. The order of the band gap is **PFDTTP** < **PFDTBT** < **PFDDTQ** < **PFTT**, which is on the reverse trend of luminescence and FET mobility. The strong acceptor strength of thieno[3,4-b]pyrazine (**TP**) and coplanar backbone in **PFDTTP** probably resulted in a high intramolecular charge transfer and led to the lowest band gap and highest FET mobility among the four polymers. The present study suggested the importance of the acceptor structure on the electronic and optoelectronic properties of semiconducting polymer based devices.

Five small band gap thiophene(**TH**)-thienopyrazine(**TP**) conjugated copolymers are successfully synthesized and characterized. Both experimental and theoretical results suggest that the band gaps reduce as the thiophene moiety increased. The relatively small optical (0.97 eV) and electrochemical (0.78 eV) band gaps of poly **PTHTP-C12** suggest the importance of intramolecular charge transfer. The theoretical geometry analysis indicates that the bond length alternation increases with the increasing the thiophene moiety and results in the above trend on

band gaps. The theoretical results also suggest that the poly(**TH-alt-TP**) could have a relatively small effective mass for field transistor applications. Our study demonstrates the tuning of the electronic properties of small band gap copolymers by the thiophene content and intramolecular charge transfer.

6. Reference

- [1] Q. Hou, Y. S. Xu, W. Yang, M. Yuan, J. B. Peng, Y. Cao, *Journal of Materials Chemistry* **2002**, *12*, 2887.
- [2] W. C. Wu, W. Y. Lee, W. C. Chen, *Macromolecular Chemistry and Physics* **2006**, *207*, 1131.
- [3] W. C. Wu, C. L. Liu, W. C. Chen, *Polymer* **2006**, *47*, 527.
- [4] Q. Hou, Q. M. Zhou, Y. Zhang, W. Yang, R. Q. Yang, Y. Cao, *Macromolecules* **2004**, *37*, 6299.
- [5] A. P. Kulkarni, Y. Zhu, S. A. Jenekhe, *Macromolecules* **2005**, *38*, 1553.
- [6] W. C. Wu, W. Y. Lee, C. L. Pai, W. C. Chen, C. S. Tuan, J. L. Lin, *Journal of Polymer Science Part B-Polymer Physics* **2007**, *45*, 67.
- [7] P. Herguch, X. Z. Jiang, M. S. Liu, A. K. Y. Jen, *Macromolecules* **2002**, *35*, 6094.
- [8] R. D. Champion, K. F. Cheng, C. L. Pai, W. C. Chen, S. A. Jenekhe, *Macromolecular Rapid Communications* **2005**, *26*, 1835.
- [9] T. Yamamoto, T. Yasuda, Y. Sakai, S. Aramaki, A. Ramaw, *Macromolecular Rapid Communications* **2005**, *26*, 1214.
- [10] Y. Zhu, R. D. Champion, S. A. Jenekhe, *Macromolecules* **2006**, *39*, 8712.
- [11] F. L. Zhang, W. Mammo, L. M. Andersson, S. Admassie, M. R. Andersson, L. Inganas, S. Admassie, M. R. Andersson, O. Ingands, *Advanced Materials* **2006**, *18*, 2169.
- [12] W. C. Wu, W. C. Chen, *Journal of Polymer Research* **2006**, *47*.

Table 1. Photoluminescence and Electroluminescence^a characteristics of Ternary blends

| | Composition(wt%) FQTP- PF:PFQ:PFTP FBTTP- PF:PFBT:PFTP | Photoluminescence | | Electroluminescence | | | | | | |
|---------------|--|--------------------------------------|---------------------------|---------------------|--------------------------------------|------------------------------------|--|------------------------------|----------------------------------|------------|
| | | $\lambda_{\max}^{\text{PL}}$ (nm) | Φ^{PL} (%) | Bias (V) | $\lambda_{\max}^{\text{EL}}$ (nm) | Brightness (cd/m ²) | Current Density ^b (mA/cm ²) | Luminance yield (cd/A) | CIE 1931 coordinates (x,y) | EQE (%) |
| FQTP1 | 98.50:1.00:0.50 | 426, 455, 474 | 30.1 | 9.5 | 430*, 477, 620 | 326 | 72.7 | 0.45 | (0.328, 0.310) | 0.13 |
| FQTP2 | 98.00:1.00:1.00 | 425, 451, 472, 615* | 21.4 | 10 | 493, 604 | 146 | 54.7 | 0.27 | (0.410, 0.302) | 0.08 |
| FQTP3 | 97.00:1.00:5.00 | 421, 444, 474*, 630, 653 | 6.03 | 16 | 450*, 639, 655 | 13 | 29.6 | 0.04 | (0.628, 0.291) | 0.06 |
| FQTP4 | 94.25:5.00:0.50 | 423, 478 | 27.5 | 12 | 482, 619 | 97 | 48.3 | 0.20 | (0.297, 0.380) | 0.08 |
| FQTP5 | 94.00:5.00:1.00 | 424, 478, 627, 655* | 19.2 | 12.5 | 489, 603 | 75 | 45.2 | 0.17 | (0.395, 0.341) | 0.07 |
| FQTP6 | 90.00:5.00:5.00 | 423, 478, 631, 654 | 5.22 | 16.5 | 477, 637, 654 | 10 | 30.1 | 0.03 | (0.580, 0.293) | 0.05 |
| FBTTP1 | 99.65:0.05:0.30 | 423, 445, 521 | 38.7 | 8 | 424, 446, 478, 513, 618* | 1360 | 72.2 | 1.88 | (0.320, 0.327) | 0.47 |
| FBTTP2 | 98.95:0.05:1.00 | 423, 445, 520, 610* | 27.6 | 9.5 | 424, 449, 476, 515, 626 | 189 | 23.4 | 0.81 | (0.502, 0.345) | 0.31 |
| FBTTP3 | 99.60:0.10:0.30 | 424, 445, 522 | 36.4 | 8 | 445, 520 | 1250 | 82.5 | 1.52 | (0.322, 0.345) | 0.45 |
| FBTTP4 | 98.90:0.10:1.00 | 423, 444, 521, 610* | 29.2 | 9.5 | 445, 520, 630 | 163 | 20.1 | 0.81 | (0.476, 0.367) | 0.30 |
| FBTTP5 | 98.50:0.50:1.00 | 423, 445, 524 | 25.1 | 9.5 | 446*, 526, 620* | 145 | 31.7 | 0.46 | (0.399, 0.466) | 0.38 |
| FBTTP6 | 95.50:0.50:4.00 | 419, 442, 526, 614 | 7.05 | 14 | 444*, 637, 654 | 14 | 28.3 | 0.05 | (0.617, 0.307) | 0.08 |

a: Device structure: ITO/PEDOT:PSS/emissive layer/Ca:Ag; measured at maximum luminance yield.

b :Active area is 0.1256 cm².

* emission shoulders

Table 2. The Electronic and Optoelectronic Properties of PFTT, PFDDTQ, PFDTBT, and PFDDTTP.

| | $\lambda_{\max}^{\text{abs}}$ (nm) | E_g^{opt} (film) (eV) ^a | $\lambda_{\max}^{\text{PL}}$ (film) (nm) | HOMO (eV) | LUMO (eV) | E_g^{ec} (eV) | Mobility (cm ² v ⁻¹ s ⁻¹) | on/off | RMS (nm) |
|----------------|------------------------------------|--|---|--------------|--------------------|------------------------|--|-----------------|-------------|
| PFTT | 484, 514 | 2.05 | 574 | -5.08 | -3.03 ^b | - | 2.35×10^{-6} | 1×10^3 | 1.155 |
| PFDDTQ | 374, 502 | 1.94 | 438, 462, 620 | -5.03 | -3.23 | 1.80 | 5.44×10^{-6} | 1×10^3 | 3.352 |
| PFDTBT | 422, 618 | 1.69 | 438, 677 | -5.06 | -3.29 | 1.77 | 4.87×10^{-5} | 2×10^4 | 1.078 |
| PFDDTTP | 416, 616 | 1.68 | 437, 736 | -4.97 | -3.76 | 1.21 | 5.52×10^{-5} | 5×10^3 | 0.472 |

^a. Estimated from the absorption edge of the thin film.

^b. LUMO = band gap^{opt} – HOMO.

Table 3. Optical absorption and electrochemical properties of the studied polymers.

| | λ_{\max} | λ_{\max} | E_g^{opt} (eV) | Oxidation (vs SCE) | | | Reduction (vs SCE) | | | E_g^{ec} (eV) ^b |
|------------------|-------------------|------------------|----------------------------|--------------------|--------------------|-------|--------------------|--------------------|-------|--|
| | solution | thin film | | E_{pa} | E_{onset} | HOMO | E_{pc} | E_{onset} | LUMO | |
| | (nm) ^a | (nm) | | (V) | (V) | (eV) | (V) | (V) | (eV) | |
| PTHTP-C7 | 748 | 790 | 1.07 | 0.52 | 0.05 | -4.45 | -1.39 | -1.15 | -3.25 | 1.20 |
| PTHTP-C12 | 774 | 850 | 0.97 | 0.85 | 0.30 | -4.70 | -0.84 | -0.48 | -3.92 | 0.78 |
| PBTHTP | 610 | 670 | 1.38 | 0.37 | 0.15 | -4.55 | -1.44 | -1.19 | -3.21 | 1.34 |
| PTTHTP | - | 640 | 1.66 | - | - | - | - | - | - | - |
| PQTHTP | - | 590 | 1.78 | - | - | - | - | - | - | - |

^a The absorption maximum in chloroform solution.

^b The electrochemical band gap, $E_g^{\text{ec}} = \text{LUMO} - \text{HOMO}$.

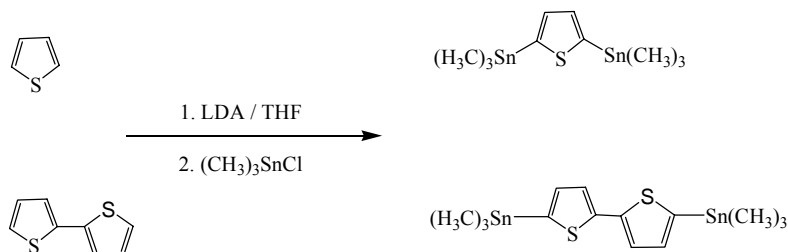
Table 4. Geometries and electronic properties of studied conjugated polymers

| Polymer | L_B^a | δ_D^b | δ_A^b | HOMO | LUMO | E_g | Effective mass | Effective mass |
|---------------|---------|--------------|--------------|-------|-------|-------|----------------|----------------|
| | (Å) | (Å) | (Å) | (eV) | (eV) | (eV) | m_H | m_L |
| PTH | 1.441 | 0.031 | - | -4.62 | -2.55 | 2.07 | -0.150 m_e | 0.164 m_e |
| PTP | 1.373 | - | 0.026 | -4.40 | -3.07 | 1.32 | -0.154 m_e | 0.242 m_e |
| PTHTP | 1.426 | 0.005 | 0.030 | -4.20 | -3.30 | 0.90 | -0.100 m_e | 0.111 m_e |
| PBTHTP | 1.429 | 0.016 | 0.037 | -4.36 | -3.15 | 1.21 | -0.103 m_e | 0.139 m_e |
| PTTHTP | 1.430 | 0.019 | 0.038 | -4.42 | -3.06 | 1.36 | -0.117 m_e | 0.165 m_e |
| PQTHTP | 1.431 | 0.021 | 0.039 | -4.46 | -3.01 | 1.45 | -0.123 m_e | 0.191 m_e |

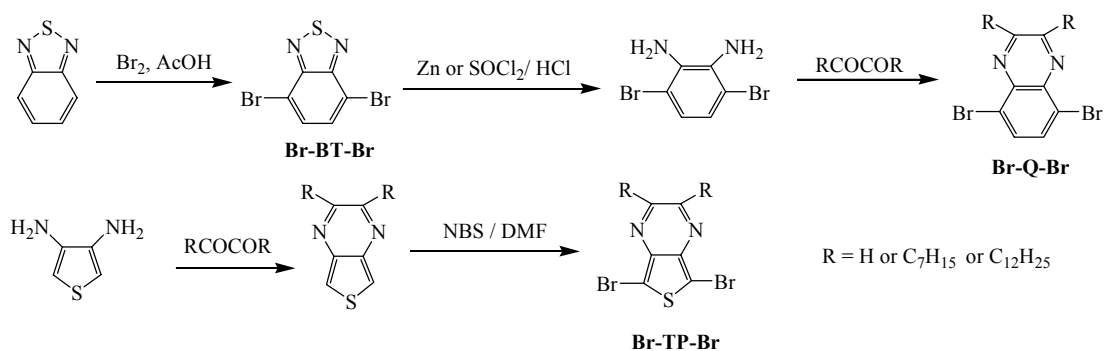
a: bridge bond length between the donor and acceptor

b: bond length between single and double bond in the donor or acceptor ring.

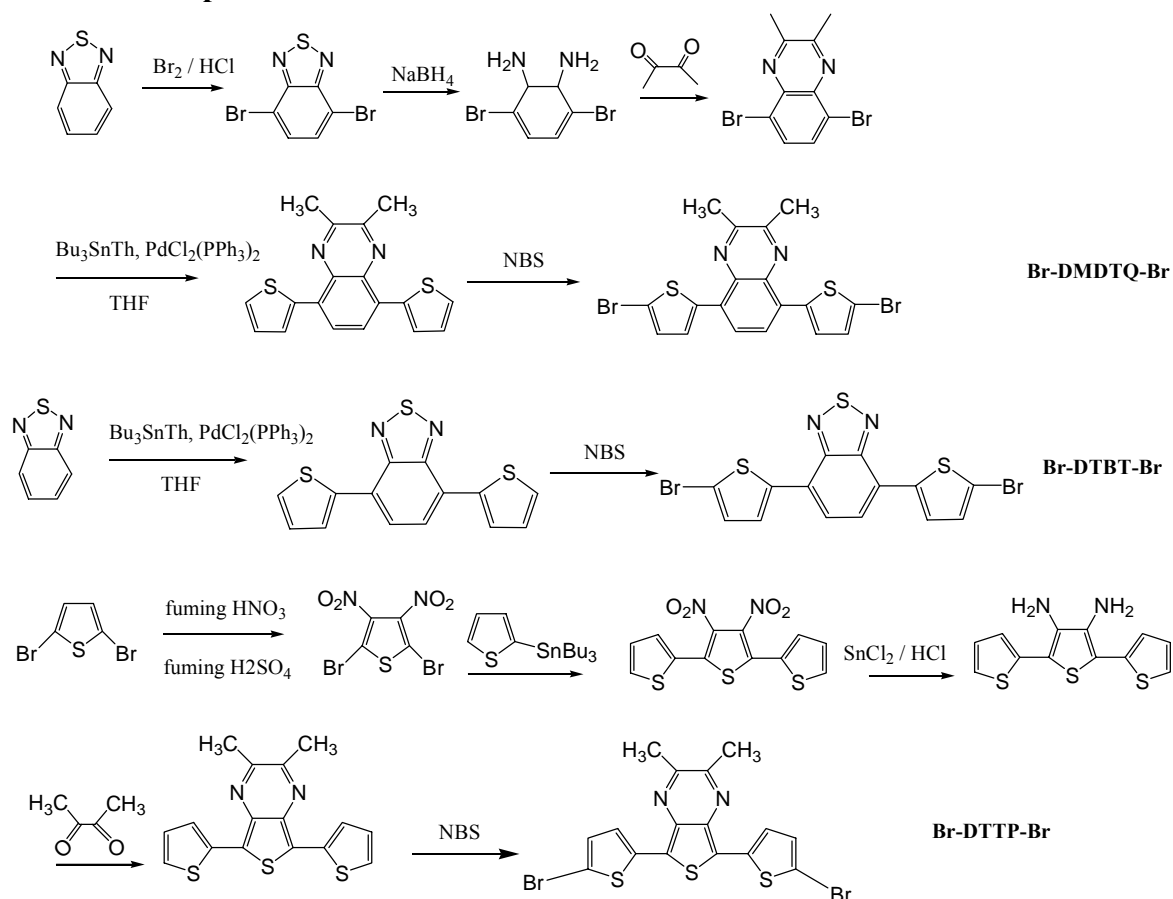
a. Thiophene Monomer



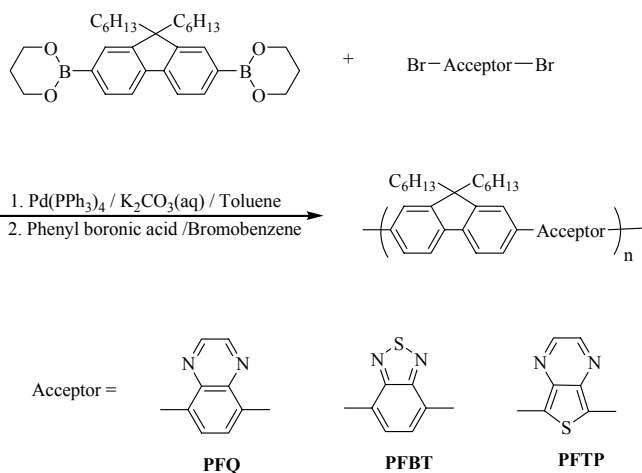
b. Acceptor Monomers



c. donor-Acceptor-donor Monomers

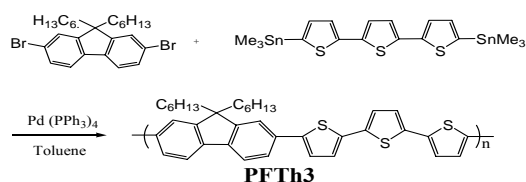


Scheme 1. The synthesis process of the monomers of thiophene, thienopyrazine, and donor-acceptor-donor moiety.

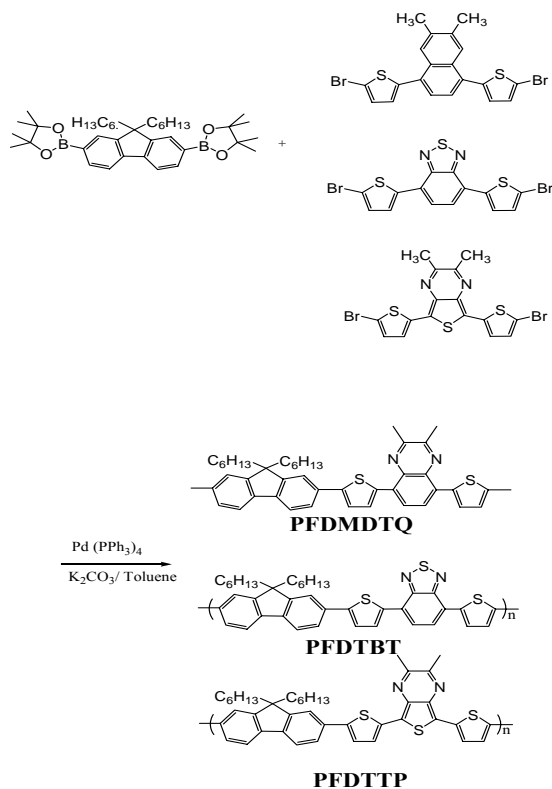


Scheme 2. Synthesis of fluorene-acceptor alternating copolymers.

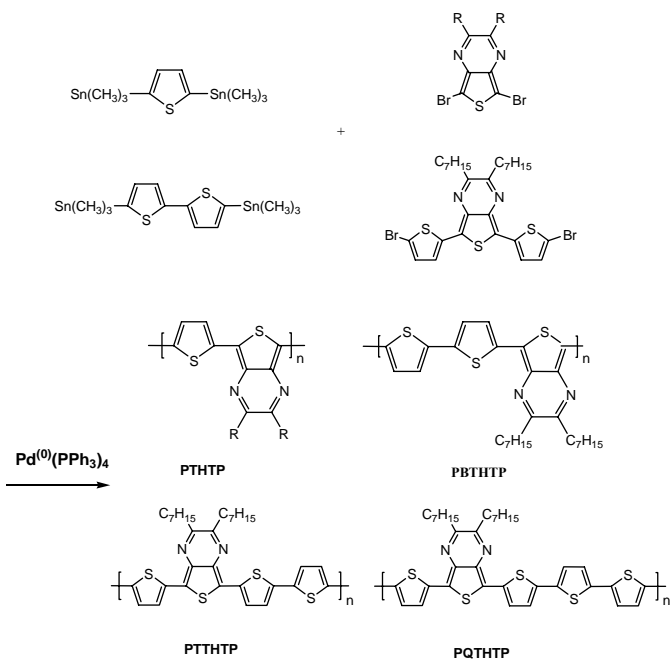
(a)



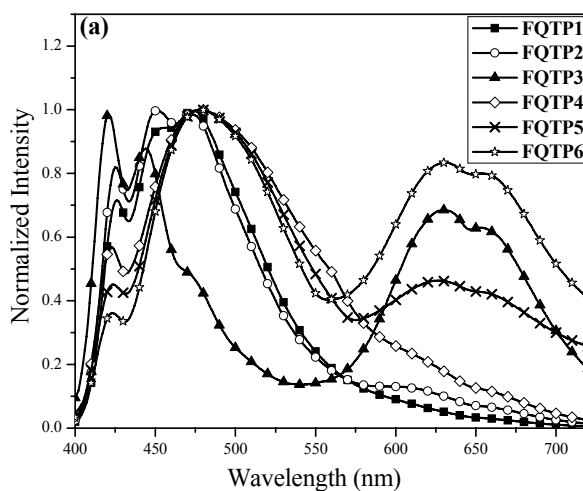
(b)



Scheme 3. Synthesis of fluorene-donor-acceptor-donor alternating copolymers.



Scheme 4. Synthetic scheme of PTTHTP and PQTHTP.



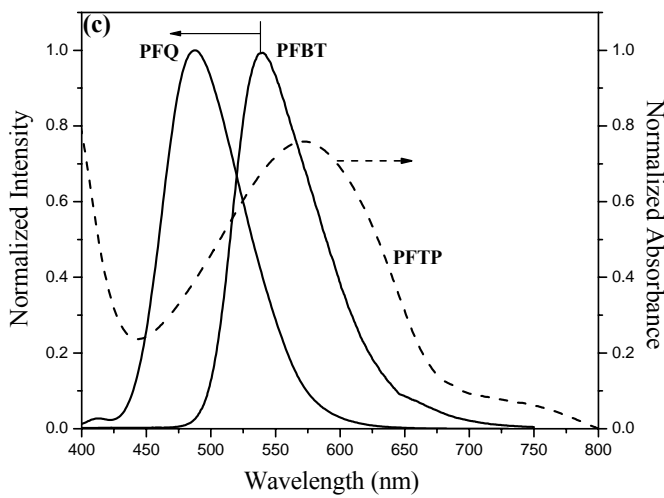
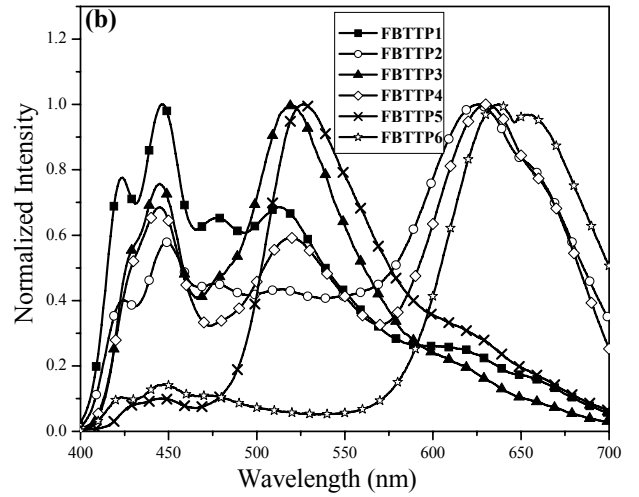
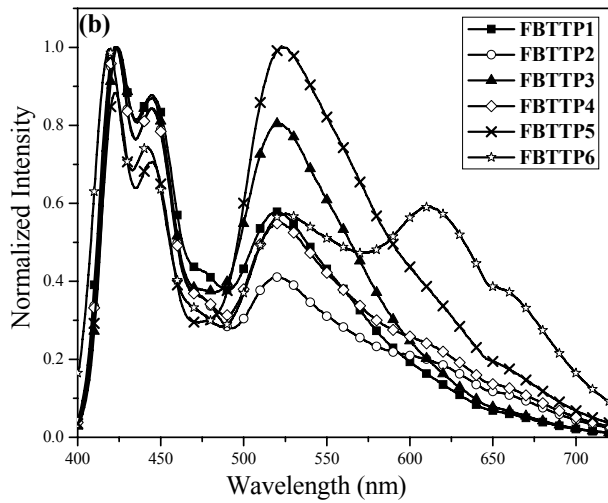


Figure 2. Normalized EL spectra of ternary the blends using (a) FQTP and (b) FBTTP as the emissive layer.

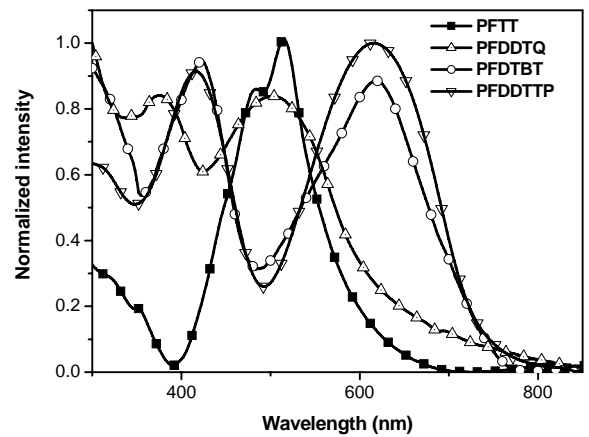


Figure 1. (a) Normalized PL of FQTP; (b) normalized PL of FBTTP; (c) PL spectra of PFQ and PFBT (solid lines) and UV spectra of PFTP.

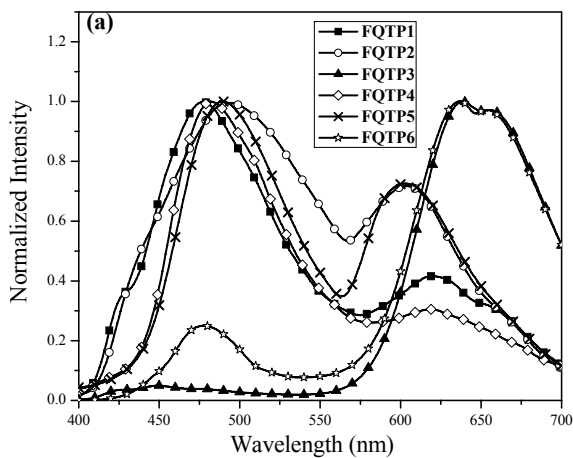


Figure3. Normalized UV-vis absorption spectra of PFTT, PFDDTQ, PFDTBT, and PFDDTTP thin films on glass substrate.

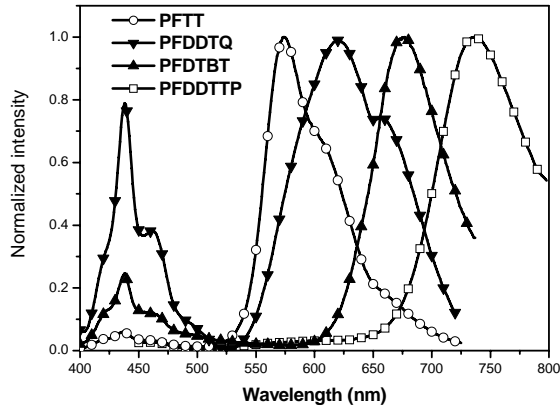


Figure 4 Normalized PL spectra of **PFTT**, **PFDDTQ**, **PFDTBT** and **PFDDTTP** in thin films on glass substrate.

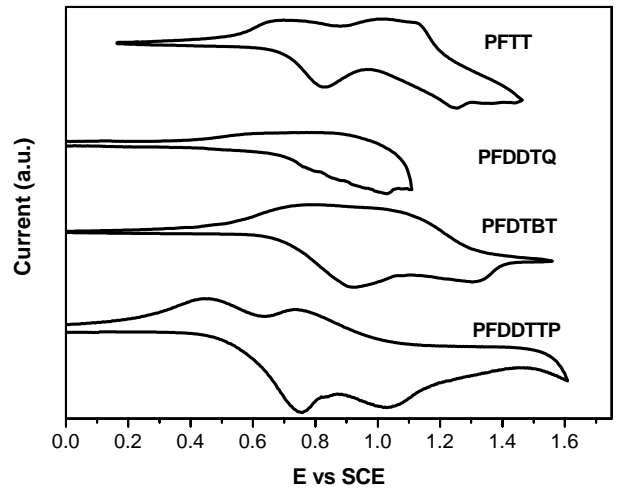
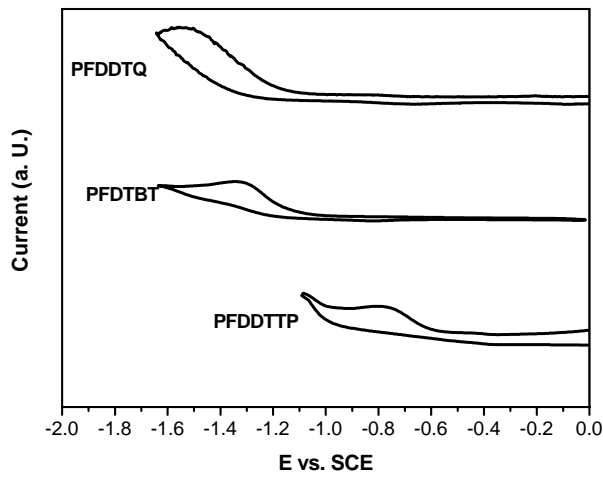


Figure 5. Electrochemical (a) reduction and (b) oxidation of cyclic voltammograms of **PFTT**, **PFDDTQ**, **PFDTBT**, and **PFDDTTP** films on a Pt electrode in acetonitrile solution containing TBABF₄ as the electrolyte.

(a)



(b)

(a)

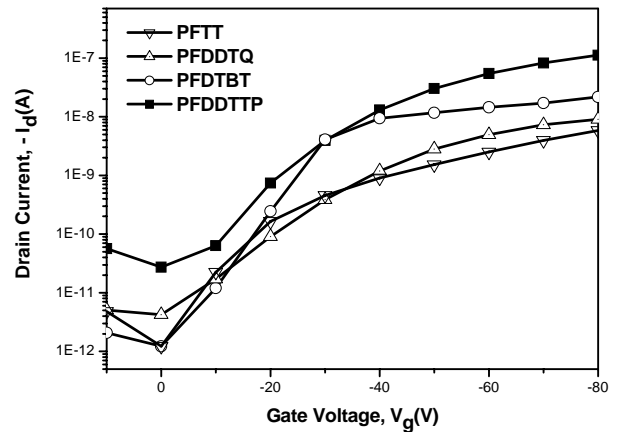


Figure 6 The transfer characteristics of **PFTT**, **PFDDTQ**, **PFDTBT** and **PFDDTTP** at $V_d = -80$ V in the saturation region, respectively.

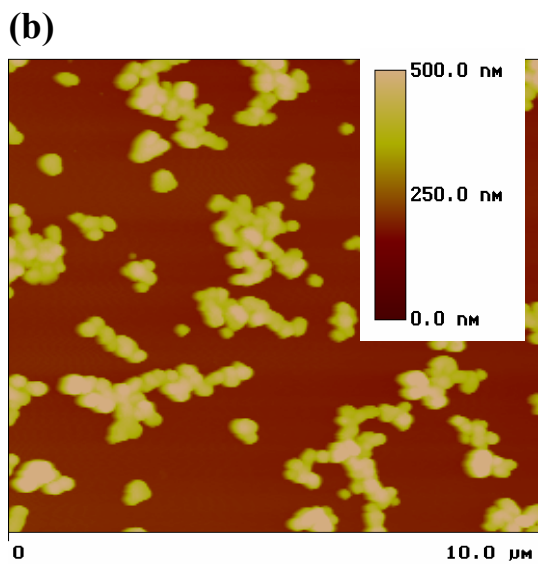
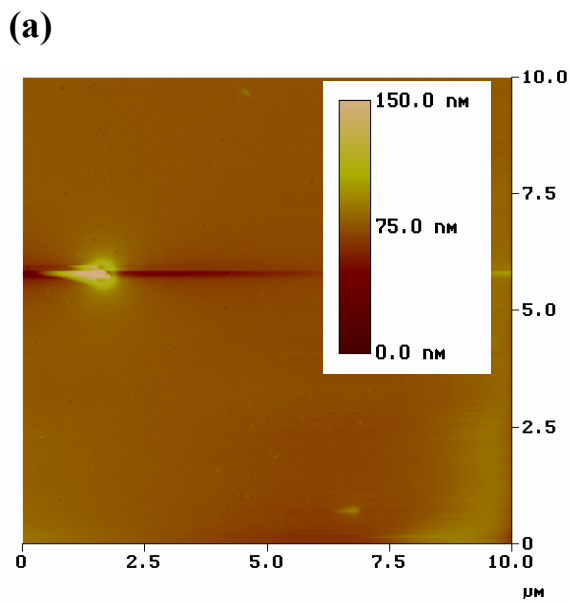


Figure 7. Topographical AFM images of **PFDDTTP** thin films obtained from various solvents: (a) 1,2-dichlorobenzene and (b) THF.

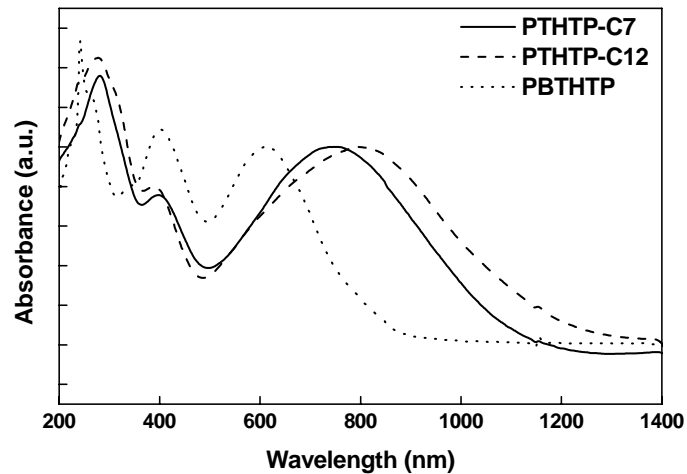


Figure 8. Optical absorption spectra of the studied copolymers in chloroform.

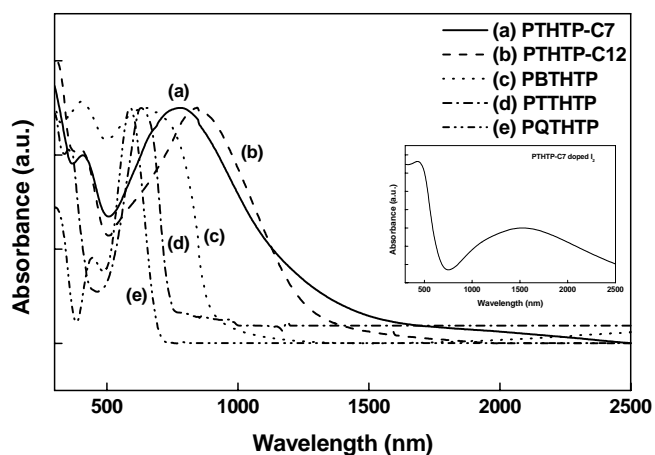


Figure 9. Optical absorption spectra of the studied copolymer films on quartz substrates.

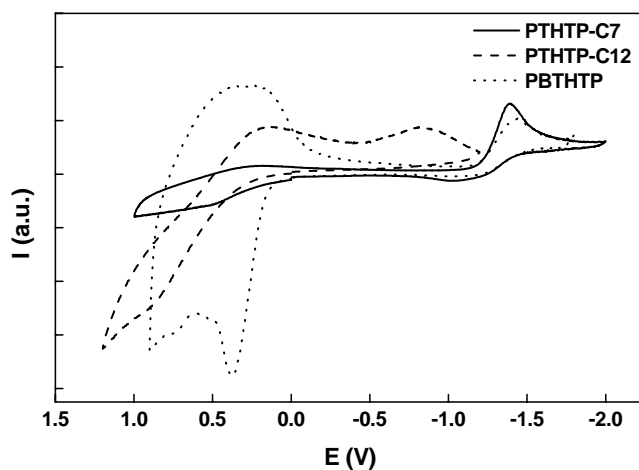


Figure 10. Cyclic voltammetry diagrams of (a) **PTHTP-C7**, **PTHTP-C12** and **PBTHTP** using the electrolyte of 0.1 M acetonitrile (99.5+%, Tedia) solution containing tetrabutylammonium tetrafluoroborate (TBABF₄).

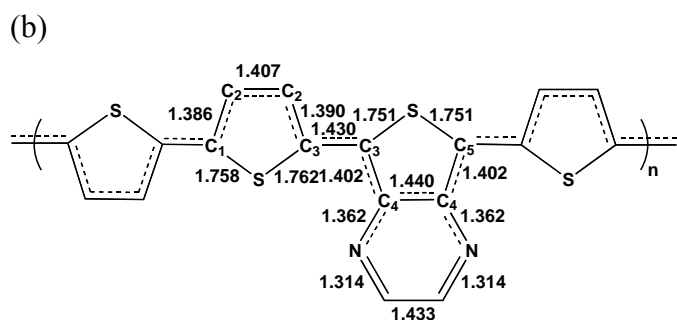
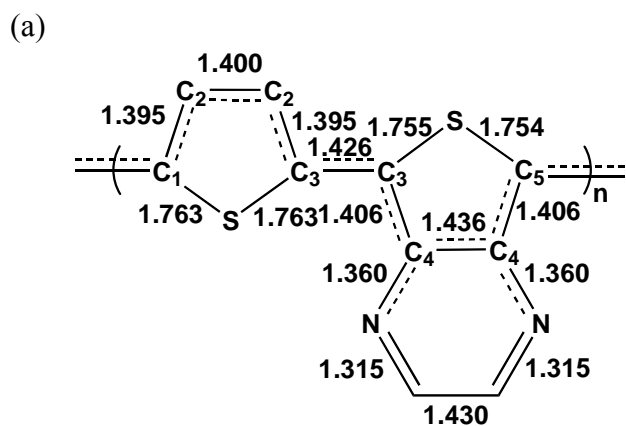


Figure 11. DFT//B3LYP/6-31G(d) optimized bond length of (a) **PTHTP** (b) **PTTHTP**.

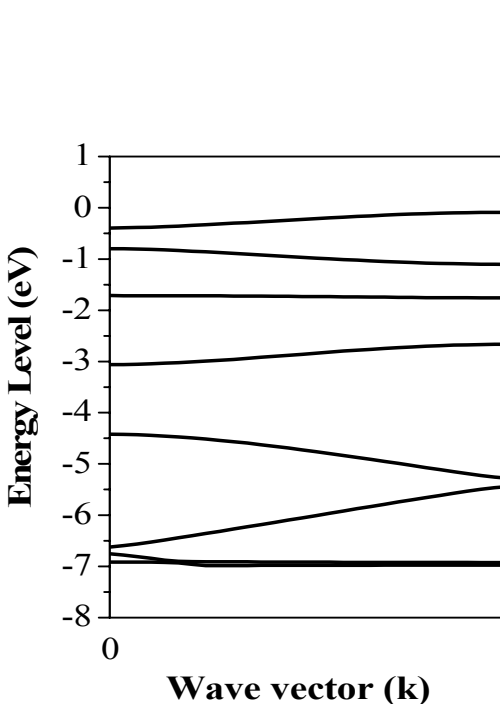
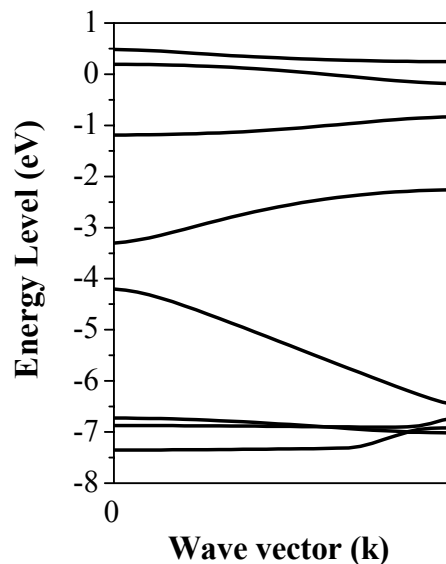


Figure 12. Band structures of (a) **PTHTP** (b) **PTTHTP** by DFT//B3LYP/6-31G(d) theory .

7、計畫結果自評

1. 本研究研究成果與原設定計畫目標相符

| 研究目標 | 研究成果 |
|---|--|
| 完成利用理論分析估算donor-acceptor共軛高分子的性質，包括geometry (bond length, bond angle, torsion angle)、electronic structure (HOMO, LUMO, Eg, BW, effective mass)。 | 以Density Function Theory配合適當之Energy Basis計算出donor-acceptor共軛高分子之最適化幾何結構與電子結構特性。並歸納出不同Thiophene-Thienopyrazine比例對其光電性質之影響。 |
| 完成共軛高分子單體合成，包括thiophene單體與一系列之acceptor單體。 | 利用適合之反應物與反應條件合成出適用於製備donor-acceptor共軛高分子之單體。 |
| 完成共軛高分子合成，包括fluorene-based copolymers 及 fluorene-based donor-acceptor-donor copolymers 及 thiophene-thienopyrazine alternating copolymers。 | 利用 Suzuki coupling 與 Stille coupling 分別成功合成 fluorene-based copolymer, fluorene-based donor-acceptor-donor copolymer 及 thiophene-thienopyrazine alternating copolymer。 |
| 完成共軛高分子之電化學、與光物理性質鑑定，包括分子量、HOMO/LUMO level、band gap、與發光特色等，並建立化學結構對共軛高分子性質的關係。 | 利用 CV 量測電化學性質、利用 UV 與 PL 量測光物理性質，建立 acceptor 強度與含量對 donor-acceptor 性質（如電子結構特性、吸收與發射波長）之關係。 |
| 完成元件之製備與性質量測，包括將 fluorene-based 共聚高分子應用於高分子發光二極體、以及將 thiophene-based 與 fluorene-based donor-acceptor-donor 共聚高分子應用於場效應薄膜電晶體。 | 將 fluorene-based 共聚高分子摻混應用於高分子發光二極體之製備，並成功製備出白光發光二極體；成功合成出低能隙 Thiophene-Thienopyrazine 共聚高分子，並成功地結合理論計算分析釐清結構與電子特性之間的關係；成功測量出 fluorene-based donor-acceptor-donor 共聚物的場效應薄膜電晶體特性，並作進一步的分析。 |

8、本年度(2006/8/1~迄今)經由本計畫經費支持共發表9篇SCI期刊論文，目錄如下。

- (1) Y. C. Tung, W. C. Wu, and W. C. Chen,* “Morphological Transformation and Photophysical Properties of Rod-Coil Poly[2,7-(9,9-dihexylfluorene)]-block-poly(acrylic acid) (PF-*b*-PAA) in Solution”, *Macromol. Rapid Commun.*, 27, 1838-1844 (2006).
- (2) C. C. Yang, Y. Tian, Alex K.-Y. Jen,* and W. C. Chen,* “New Environmental-Responsive Fluorescent NIPAA Copolymer and Its Application on DNA Sensing”, *J. Polym. Sci. Polym. Chem.*, 44, 5495-5504 (2006).
- (3) G. S. Liou,* S. H. Hsiao, W. C. Chen, and H.

J. Yen, "A New Class of High T_g and Organosoluble Aromatic Poly(amine-1,3,4-oxadiazole)s Containing Donor and Acceptor Moieties for Blue Light-Emitting Materials", *Macromolecules*, 39, 6036-6045.(2006) (4)W. C. Wu, W. Y. Lee, C. L. Pai, W. C. Chen^{*}, C. S. Tuan, and J. L. Lin, "Photophysical and Electroluminescent Properties of Fluorene Based Binary and Ternary Donor-Acceptor Polymer Blends", *J. Polym. Sci. B: Polym. Phys.*, 45, 67-78(2007). (5). W. C. Wu, Y. Tian, C. Y. Chen, C. S. Lee, Y. J. Sheng, W. C. Chen^{*} and Alex K.-Y. Jen,^{*} "Theoretical and Experimental Studies on the Surface Structures of Conjugated Rod-Coil Block Copolymer Brushes", *Langmuir*, 23, 2805-2814(2007). (6) H. Y. Lin, G. S. Liou,^{*} W. Y. Lee, and W. C. Chen^{*}, " Poly(triarylamine):Synthesis, Properties, and Its Blend with Polyfluorene for White-Light Electroluminescence", *J. Polym. Sci. Polym. Chem.*, 45, 1727-1736 (2007). (7) C. C. Yang, Y. Tian, C. Y. Chen, Alex K.-Y. Jen^{*} and W. C. Chen^{*}, "A Novel Benzoxazole-containing Poly(*N*-isopropylacrylamide) Copolymer as Multifunctional Sensing Materials", *Macromol. Rapid Commun.* 28, 894-899(2007). (8) A. Babel, Y. Zhu, K. F. Chen, W. C. Chen, and S. A. Jenekhe,^{*} "Morphology, High electronic Mobility, and Ambipolar Charge Transport in Binary Blend of Donor and Acceptor Conjugated Polymers", *Adv. Funct. Mater.*, in press (2007). (9) G. S. Liou,^{*} Y. L. Yang, W. C. Chen, Y. L. Oliver Su, "4-Methoxy-substituted Poly(triphenylamine):A P-type Polymer with Highly Photoluminescence and Reversible Oxidative Electrochromic Characteristics", *J. Polym. Sci. Polym. Chem.*, in press.

參加 2007 年 American Chemical Society 233rd National Meeting & Exposition

報告人：闕居振(本計畫出國經費乃支持包括我在內
實驗室三位博士班發表論文之出國差旅費)
台大化工所/高分子所

一、參加會議過程

筆者有幸於 3/24~3/29 之間參與 American Chemical Society (ACS)所舉辦的 233rd National Meeting & Exposition。American Chemical Society 為國際上最大的化學協會，其中共分成三十三個 technical division，並邀請許多國際學者參與討論，包含諾貝爾獎得主 Alan J. Heeger 等等知名教授。據大會統計，參與人數高達一萬兩千人以上，口頭與海報發表篇數也將近九千七百多篇，是國際少見的大型會議。在筆者所參與 Polymer Chemistry Session 中，許多國內各大學亦有許多為學者受到邀請口頭報告，並且在壁報展覽會場中，亦有許多國內研究成果發表，充分顯示我國在高分子化學領域的研究實力。本實驗室除我之外，另有李文亞及童宜峙發表口頭或壁報論文，題目如下：

1. Chu-Chen Chueh, Wen-Ya Lee, Kai-Fang Cheng and Wen-Chang Chen, "Synthesis and Optoelectronic Properties of Poly(quinoxaline vinylene) and Its Random Copolymer with Fluorene".
2. Wen-Ya Lee, Kai-Fang Cheng, Then-Fu Wang, Chu-Chen Chueh, Wen-Chang Chen, Chih-Shen Tuan, and Jen-Lien Lin, "Effects of Acceptors on the Electronic and Optoelectronic Properties of Fluorene Based Donor-Acceptor-Donor Copolymers".
3. Yi-Chih Tung, Wen-Chung Wu, Wen Chang Chen, "Morphological Transformation and Photophysical Properties of Fluorene Based Rod-Coil Copolymers in Solution".

二、與會心得與建議

由於筆者本身致力於高分子光電元件材料之製備與研究，因此對於 Polymer Chemistry 與 Polymer Materials: Science & Engineering 領域感到相當興趣。尤其是 Polymer Chemistry 次領域，由於剛好是共軛高分子三十週年，因此此領域有一專題就是 30 years of Conducting polymers，邀請了許多國內外知名學者來演講，如聖塔芭芭拉大學的諾貝爾獎得主 Alan J. Heeger、西雅圖華盛頓大學的 Jenekhe 以及研究小分子場效應電晶體的史丹福大學 Bao 等等著名教授都是本次會議邀請的重點。共軛有機物與高分子由於是新的科學領域，因此有許多潛力需要去發掘，為了進一步地提升有機材料於光電元件上的應用，許多學者在此會議上提出一些新的議題激發大家的靈感。

如諾貝爾獎得主 Alan J. Heeger 發表一系列利用共軛高分子所製備成的 Light Emitting Field-Effect Transistor，此元件利用高分子之 ambipolar 特性，同時在元

件中注入電洞與電子，利用電場大小控制元件發光位置，進一步發掘共軛高分子於業界的應用潛力。

由於 Pentacene 小分子在空氣中的穩定性不佳，而且此材料只能利用高費用的蒸鍍機製備，在商業化上遭遇到不少困難。史丹福大學的 Bao 教授為了提升 Pentacene 的應用性，特別將 Pentacene 與各種不同的單體共聚合成高分子，以提升其材料的可塗佈性與大氣穩定性，開創了全新的共軛分子研究領域。這方面的研究與本實驗室所研究的主題相關，未來如何將 Pentacene 與 donor/acceptor 系統結合就是實驗室未來可以努力的方向。

國際上高分子太陽能電池的領先者 Yang Yang 教授在研發有機光電元件上有更新的突破，他們實驗室利用 poly(3-hexyl-thiophene)/Au nanoparticles 以及 polyaniline nanofiber/tobacco mosaic virus 等等不同的 polymer/biomolecule(或是 polymer/ nanoparticle) 摻混物製備出全新的高性能有機記憶體元件，擁有很快的資料擷取速度 (< 1microsecond)。不過其中，他也提到此元件在穩定性方面並無法與目前的記憶體元件相比，因此如何提升有機元件在這方面的穩定性是未來可以繼續研究的課題。目前有機光電元件的研究主要在於場效應電晶體、有機發光二極體與太陽能電池上，想要在這方面上比其他國外實驗室有更大的突破並不是件容易的事情，但在有機記憶體元件上，國內外投入的學者並不多，或許是一個新的契機可以去努力的。

國內在有機光電元件的研究上其實並不遜於國外學者，無論在效能與製程上都可以達到國外研究的水準，但是要如何找到適當的研究主題切入以及如何研發具有原創性的研究就是需要國內學術界更加倍的努力了。

三、攜回資料

2007 American Chemical Society 233rd National Meeting & Exposition 會議論文、摘要及相關資料

四、致謝

此次承蒙國科會補助出國開會，特此感謝